Digital analysis of the geometric variability of Guadua, Moso and Oldhamii bamboo

Rodolfo Lorenzo[1*], Leonel Mimendi[1], Martha Godina[1] and Haitao Li[2]
[1]Department of civil, Environmental and Geomatic Engineering, University College London, London WC1E 6BT, UK
[2]College of Civil Engineering, Nanjing Forestry University, Nanjing, 210037, China
[*]Corresponding Author: Rodolfo Lorenzo, e-mail: r.lorenzo@ucl.ac.uk.

Abstract
The implementation of sustainable building materials is currently one of the principal global challenges faced by the construction industry. Natural bamboo culms are a potential alternative to tackle this challenge due to its favourable environmental credentials as well as affordability. However, the organic geometry of bamboo culms is one of the barriers that prevents them from being implemented in formal design procedures. This work presents the details of a new digitisation workflow to systematically capture the geometry of bamboo culms through the application of 3D scanning technologies and reverse engineering principles. This workflow is applied to carry out a comprehensive analysis of the geometric variability of Guadua angustifolia kunth (Guadua), Phillostachys pubescens (Moso) and Bambusa oldhamii (Oldhamii) to identify potential correlation patterns. This geometric analysis showed a wide variation in the geometric properties of all species and no particular pattern was found which could be adopted for a potential visual grading system. These results highlight the challenges that the use of bamboo culms pose for the traditional design and fabrication processes developed for manufactured structural elements. The proposed reverse engineering methodology adopted for this study can be used to quantify and manage the geometric variability of bamboo culms to support the development of new formal design and fabrication processes for this natural structural element.

Keywords: Bamboo; Geometric properties; Reverse engineering; 3D scanning; Sustainable building materials

1. Introduction
The building industry is already facing a major challenge as the production of the main construction materials is responsible for almost 50% of the global CO_2 emissions [1], therefore the urgent implementation of sustainable materials is needed to satisfy the increasing global housing demand in developing countries [2] and reach the global aim of affordable, sustainable and resilient housing [3]. In recent years, commercial organisations and research institutions have focused their attention on natural bamboo culms because of its favourable environmental properties [4,5]. Among the different bamboo products currently being explored to provide the building industry with sustainable alternative solutions, natural bamboo culms are, as expected, the alternative with the lowest environmental impact [6].

Bamboo is a woody grass endemic to tropical and sub-tropical regions with more than 1600 species [7] from which around 100 have been identified suitable as building material [8]. In spite of the potential of bamboo culms to become widely used as a sustainable resource, there are fundamental cultural and technical challenges yet to be addressed. One of the main challenges is related to the inherent variability of their geometric properties that prevent the formal design of bamboo structures and the implementation of robust construction processes to ensure high standards and quality. The main geometric features of bamboo culms are their nodes, internodes, and nodal diaphragms as shown in Fig. 1. Researchers have investigated the variation of basic geometric properties of two of the most common species: Guadua and Moso [9–11], where they have described a general pattern of diameter and thickness reduction along the length of the bamboo when measured from the bottom of the culm. These variations will consequently have an effect on the structural behaviour of the bamboo culms along with its straightness [11–13]. In these studies, different methods have been applied to acquire the basic geometric properties of bamboo culms, however they have all been based on traditional manual processes which present significant challenges to efficiently capture the complex, organic geometry of bamboo culms and collect a representative amount of data on the species suitable for construction. As a result, these manual geometry measuring processes have been applied to a limited number of bamboo culms focused on average properties [14] taken from discrete sections of the culms. In cases were the geometry of culms has been measured along their length, (outer geometry and out-of-straightness), the proposed procedures [12,15] are relatively complex and their large scale implementation poses significant challenges. The out-of-straightness ratio (δ_r) is an index commonly used to define the compression capacity for column elements and has been proposed as a grading parameter for bamboo columns [12,13]. Table 1 shows a summary of the limits that have been proposed for different bamboo species and timber. As expected, the limits for bamboo allow a larger initial deformation than for timber, however the values found in the literature can vary substantially from one species to another.

Limit ratio (δ_r)	Specie	Source
150	Dendrocalamus giganteus	Ghavami & Moreira, 2002 [12]
200 or 0.15D	Kao Jue	Yu et al 2003 [13]
100 or 0.15D	Moso	Yu et al 2003 [13]
300	Guadua	NSR-10 G, 2010 [16]
50	-	Kaminski et al, 2017 [17]
300	Sawn timber	EN 1995-1-1, 2004 [18]

Table 1. Out-of-straightness limit ratio (δ_r) for bamboo and timber

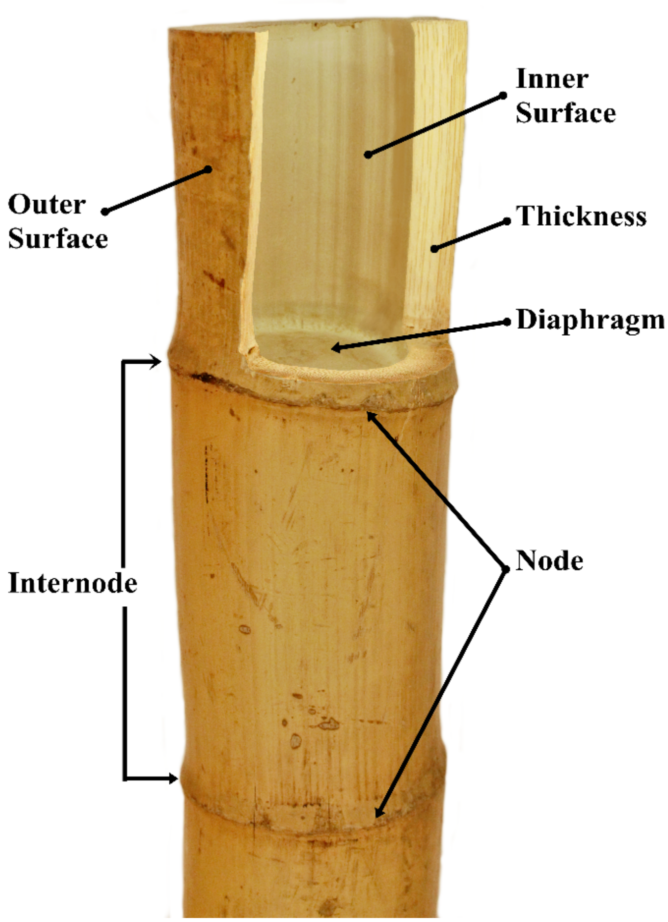

Figure 1. Basic geometric features of a bamboo culm

An alternative to perform manual measures are the non-destructive 3D scanning methods which have been broadly applied in different engineering disciplines [19–23] to acquire, quantify and, subsequently, digitally analyse the geometric properties of irregular objects, with a considerable increase in applicability, accuracy and efficiency when compared with analogue methods [24]. Therefore, a well-adapted 3D scanning process can support the acquisition of the geometric properties of bamboo to increase our understanding of its geometric variability [25] and at the same time, enable the use of highly accurate geometric data needed for the development of complex structural systems such as 3D grid-shells [26], as well as the fabrication of traditional and modern connections [27].
The objective of this work is to carry out a comprehensive analysis of the geometric variability of three different bamboo species based on the application of 3D scanning technologies and reverse engineering principles. This study follows a previously developed approach [28] for the digitisation of bamboo culms based on initial 3D polygon-mesh models [29]. These mesh models are further processed into lighter Non-uniform rational basis spline (NURBS) models [30] from which geometric properties are computed and analysed. This information is used in this study to examine the variability of each culm and identify any potential correlation patterns that could form the basis of a grading system for bamboo culms.

2. Materials and methodology

Native species from Colombia, China and Mexico were chosen for the development of this project, as described in Table 2. The average length of the culms was 2.8 meters and were extracted from the bottom section of the plant according to [14]. The culms were procured from local bamboo distributors according to local plantation management processes. All bamboo culms were kept in a controlled laboratory environment as recommended by [14], at a temperature of 23°C ±2°C and relative humidity of 55% ±5% for the duration of the digitisation process.

Species	Origin	Age (years)	Number of culms
Guadua angustifolia kunth (Guadua)	Valle del Cauca, Colombia	2 – 5	30
Phyllostachys pubescens (Moso)	Jiangsu, P.R. China	3 - 4	84

Bambusa oldhamii (Oldhamii)	Veracruz, Mexico	3 - 5	121

Table 2. General properties of bamboo culms

2.1. Digitisation process

The acquisition of the geometry was carried out with an Eva scanner from Artec 3D [31], which was used to generate a point cloud [32] of the outer bamboo surface as well as the cross section at each end of the culm and a portion of the inner surface. Fig. 2a shows the bamboo point cloud obtained at the end of the geometric data acquisition. This point cloud is subsequently processed using the proprietary software Artec Studio 12 [31] to create the corresponding 3D polygon-mesh model of a single bamboo culm. The specific details of the scanning and processing parameters are shown in Table 3 and Fig. 2b shows the final triangulation of the point cloud to create a 3D polygon-mesh of the scanned culm The average accuracy of the scanned polygon mesh was 1% for cross sectional dimensions and 1/1000th of the culm length compared with manual measurements [28]. The scanner was operated with a laptop Dell XPS 15 equipped with an Intel i7-6700HQ CPU @ 2.66GHz, 16GB of installed memory and a dedicated video card Nvidia GTX GeForce 960m with 4GB of memory whilst the processing of point cloud was carried out in a work station Dell Precision with an Intel Xeon E5-1620v3 CPU @ 3.5GHz, 32GB of memory and a dedicated video card Nvidia Quadro K2200 with 4GB of memory.

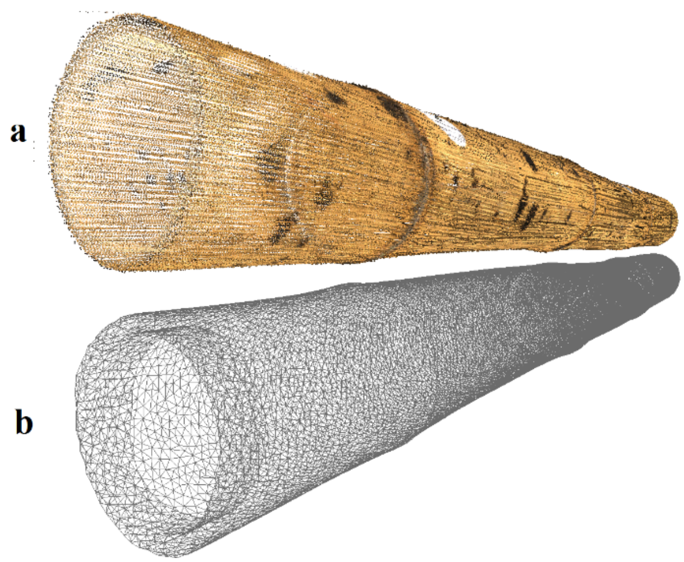

Figure 2. Point cloud (a) and polygon-mesh (b) of a typical bamboo culm

Digitisation process parameters	
Scanning	
	Scanner accuracy: 0.1 mm
	Geometry and texture acquisition
	Simultaneous rotational and translational scanning
	Acquisition at eight frames per second
Point cloud to polygon mesh	
	Fine registration (Geometry and texture)
	Global registration (Geometry and texture)
	Outlier removal (Resolution: 0.5mm)
	Fast fusion (Polygon mesh reconstruction, resolution
	Polygon-mesh simplification (Mesh accuracy: 1 mm)

Table 3. Parameters applied for bamboo digitisation process [28]

2.2. NURBS model and geometric properties

The use of a polygon mesh model to quantify the geometric properties of bamboo culms is impractical because its level of detail requires high computational resources and post-processing time to extract basic geometric properties and the prohibitive large size of a typical mesh file (approx. 50MB). For these reasons, the polygon mesh of each culm was post-processed using the extensive Rhinoceros 3D library [33] implemented in Python [34] to create a much lighter (approx. 1MB) NURBS-model of each culm. This post-processing follows basic reverse engineering principles [25] to create a digital database of bamboo culms incorporating a geometric representation of the outer and inner surfaces together with a numerical text file with all relevant geometric properties.

The identification of the polygon-mesh vertices defines the geometry of each of the nodal diaphragms (nodes) of the digital culm (Fig. 3a). These vertices are used to fit intersecting planes through each node. Similarly, an intersecting plane is fitted at each end of the culm, ensuring that both inner and outer surfaces are intersected, as seen in Fig. 3a. The asymmetric curves found from the intersection between the planes and the polygon-mesh (Fig. 3b) are modelled as NURBS-curves, defined by 20 control-points. The centroid of the outer NURBS-curves defines the centroidal line of the external bamboo surface (Fig. 3b). Additional outer NURBS-curves are obtained sectioning this surface around each node with a series of planes parallel to the original planes fit through the nodes. Similarly, the central region of each internode is sectioned with planes perpendicular to the centroidal line of the external bamboo surface. These sections are spaced two millimetres apart, covering a length of one diameter centred on each node and half a diameter centred on each internode as shown in Fig. 3b. These outer NURBS-curves are then used to fit a NURBS-surface through them. A general linear variation of the thickness along the length has been confirmed by several authors [9,10,12,35], therefore a second NURBS-surface is interpolated based on the two inner curves at each end following the centroidal axis. These two outer and inner surfaces constitute the NURBS model of a bamboo culm (Fig. 3c), with an overall deviation of 0.1 mm between the polygon mesh vertices and the NURBS surface calculated through the relevant Rhinoceros 3D function. Finally, cross-sections at each node are found by intersecting the original planes and the two NURBS-surfaces (Fig. 3c). The centroid of these cross-sections defines the true centroidal line of the bamboo culm, conservatively ignoring the solid diaphragm at each node (Fig. 3d). The nodal sections constitute the basis for the discretisation of the digital models with cross-section properties defined at the centre of each internode (Fig. 3d). A typical cross-section is shown in Fig. 4, together with an equivalent circular tube section (dashed), an arbitrary set of axes *y* & z, the actual cross-section principal axis *1* & *2* and its corresponding angle θ. Equivalent circular tube properties (diameter, thickness and inertia) are derived from the actual cross-sectional area at every internode of the bamboo model as follows:

Cross sectional area (mm^2), $A = A_{out} - A_{int}$ (1)

Equivalent diameter (mm), $D = \sqrt{\frac{4A_o}{\pi}}$ (2)

Equivalent thickness (mm), $t = \frac{D - \sqrt{D^2 - \frac{4A}{\pi}}}{2}$ (3)

Equivalent moment of inertia (mm^4), $I = \frac{\pi}{64}[D^4 - (D - 2t)^4]$ (4)

Principal moment of inertia (mm^4), $I_{1,2} = \frac{1}{2}\left[\left(I_y + I_z\right) \pm \sqrt{\left(I_z - I_y\right)^2 + 4{I_{yz}}^2}\right]$ (5)

Orientation angle (rad), $\theta = \frac{1}{2}\tan^{-1}\left(\frac{2I_{yz}}{I_z - I_y}\right)$ (6)

where A_{out} and A_{int} are the actual cross-sectional areas of the outer and inner NURBS-curves respectively, I_y, I_z & I_{yz} are the moments of inertia and product moment of inertia of the cross-section about the arbitrary orthogonal axes. The centroid coordinates of the cross-sections at the nodes were used to calculate the following:

Length of the culm (mm), $L = \sqrt{\left[\left(x_f - x_i\right)^2 + \left(y_f - y_i\right)^2 + \left(z_f - z_i\right)^2\right]}$ (7)

Internodal length (mm), $IL = \sqrt{\left[\left(x_j - x_k\right)^2 + \left(y_j - y_k\right)^2 + \left(z_j - z_k\right)^2\right]}$ (8)

where *x*, *y* & *z* are the coordinate components of the centroid, sub-indexes *i* & *f*, are the initial and final node and *j* & *k* are any two consecutive nodes. The out-of-straightness (δ) was digitally measured following the recommended methods of measurements for round and sawn timber [36]. As such, the out-of-straightness was calculated as the maximum perpendicular distance between the centroidal line of the element (Fig. 3d) and a straight line joining the centroid of the cross sections at each end.

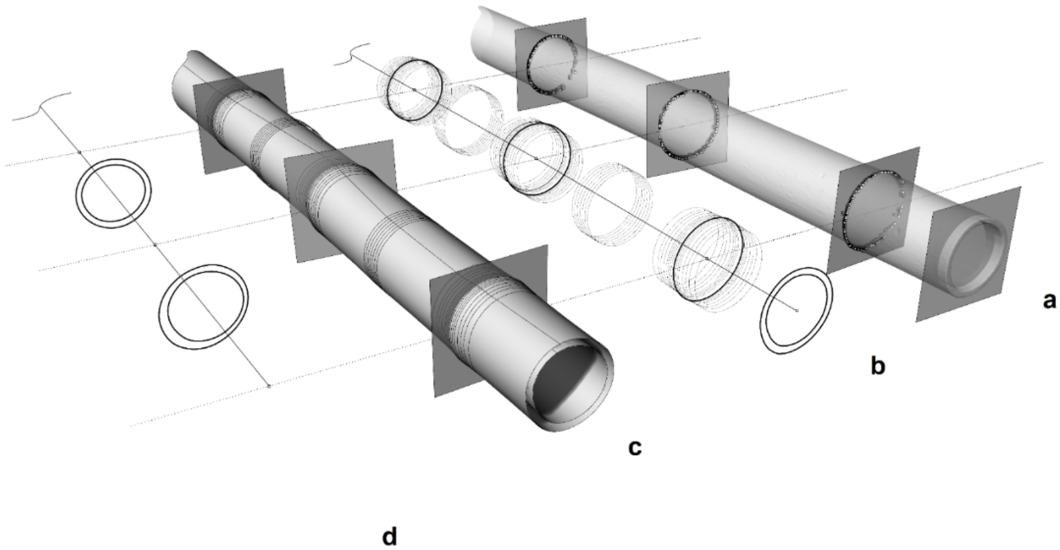

Figure 3. Polygon-mesh model (a) simplification process (b) into a NURBS-surface (c) and its corresponding discretised model (d)

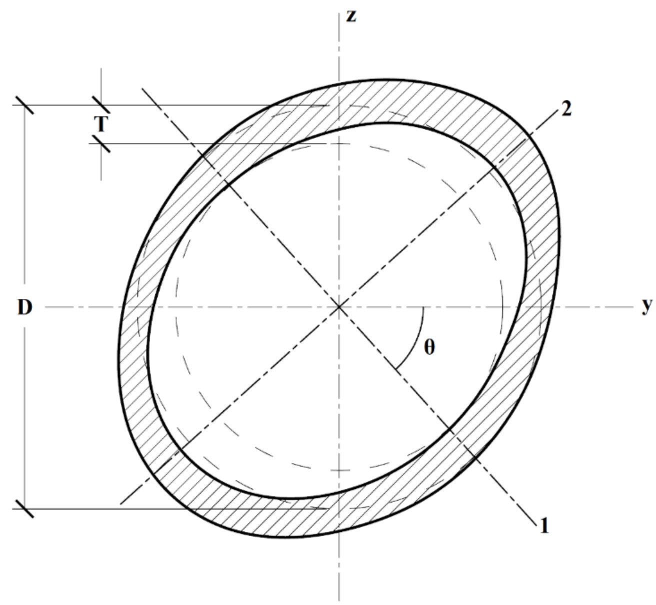

Figure 4. Typical asymmetric cross-section and its corresponding equivalent section (dashed)

3. Results

A total of 235 scanned bamboo culms were included in a digital database from which basic geometric properties were extracted, compared and analysed. Fig. 5 shows an example of a typical bamboo NURBS model and its corresponding geometric properties. In total, 250, 961 and 650 digital measurements of diameter, thickness and internodal length were extracted for Guadua, Moso and Oldhamii bamboo, respectively. A single out-of-straightness (δ) was measured for each bamboo, and it is expressed in Fig. 6 as a ratio (δ_r) of the total length to the out-of-straightness measurement:

Out-of-straightness ratio (mm/mm): $\delta_r = \frac{L}{\delta}$ (9)

Statistical values (mean, standard deviation, minimum and maximum) of these basic properties were calculated for each bamboo species and a summary of results is shown in Fig. 6 and Table 4.

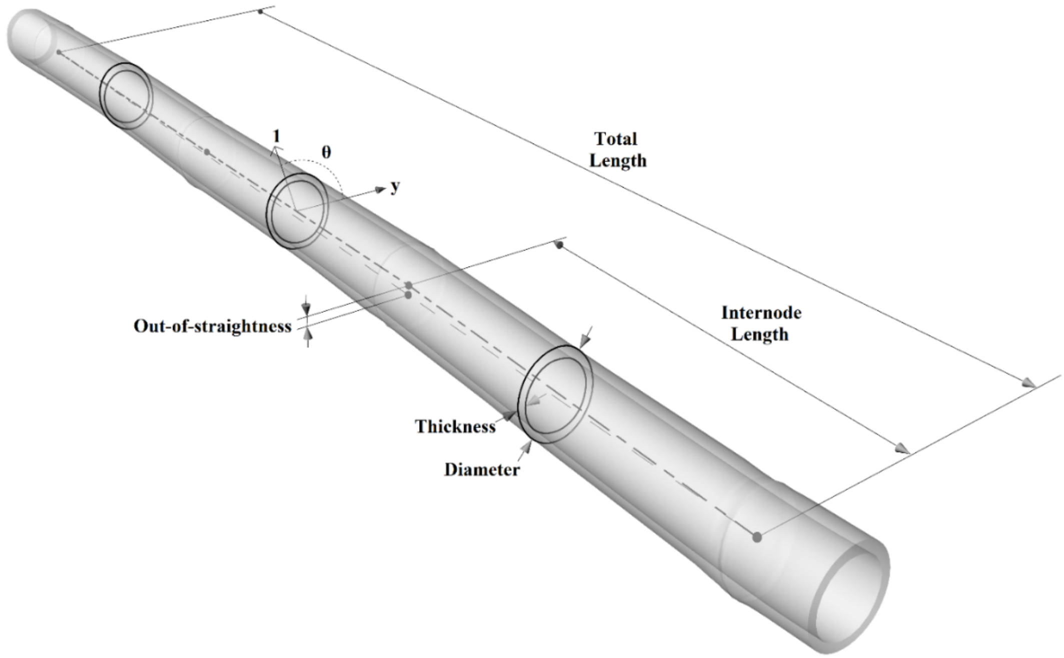

Figure 5. Typical NURBS model of a digitised bamboo culm and basic geometric properties extracted from it

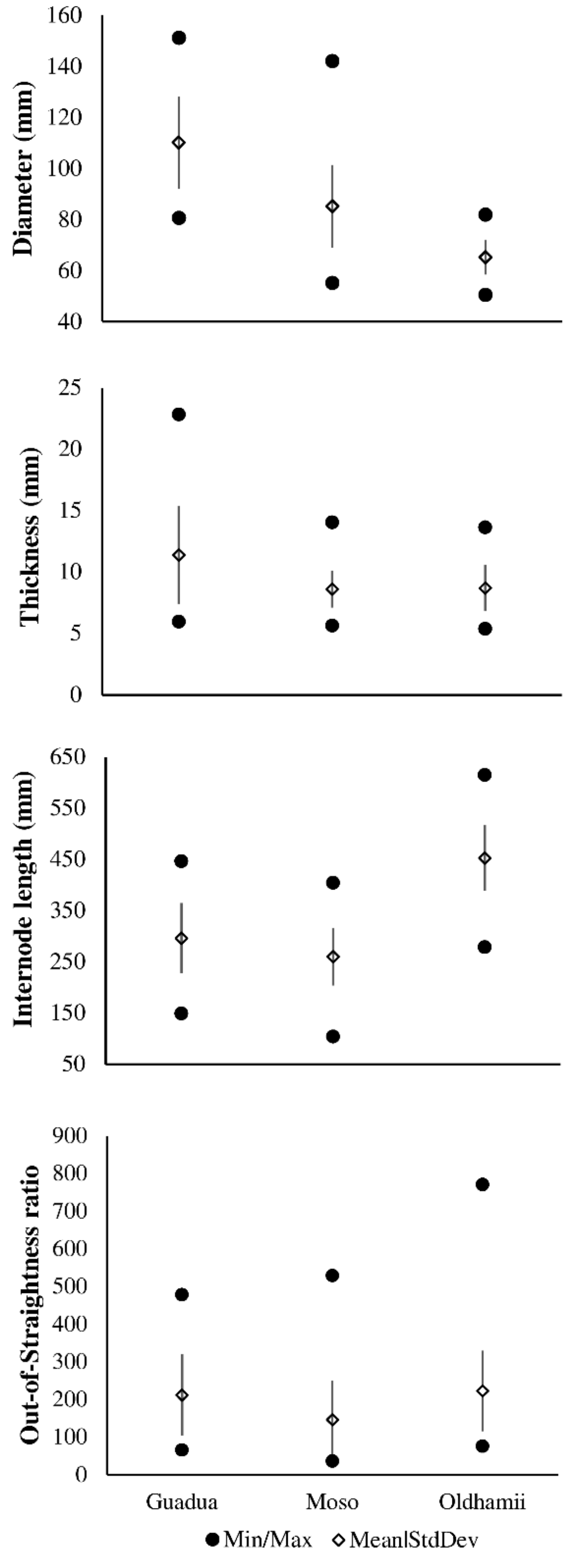

Figure 6. Mean, standard deviation and extreme values of basic geometric properties

The range of diameter for Guadua and Moso are relatively high compared to Oldhamii, which presented more consistent equivalent diameter values for the measured culms. Guadua presents the largest range in thickness but with an average value similar to those of Moso and Oldhamii. The three species presented a high variation in internodal length with Oldhamii having a higher average value than Guadua an Moso. Out of straightness ratio showed the most variable results among the studied species with Oldhamii being in average the straightest culms and Moso the species with the highest average out-of-straightness.

3.1. Cross-section properties

As displayed in Fig. 4, the actual cross-section properties of the bamboo differ compared to those of an equivalent circular tube because of bamboo's organic nature. Fig. 7 and Table 4 show the percentage difference between the moment of inertia of an equivalent circular tube (I), taken as benchmark, and the principal major (I_1) and minor (I_2) moments of inertia of the actual cross-section. Fig. 8 shows the cumulative frequency distribution related to the percentage difference between I, as benchmark, and I_1 & I_2. This figure illustrates the percentage of culms (vertical axis) whose actual moment of inertia (I_1 or I_2) differs from the idealised inertia (I) by no more than a given percentage difference (horizontal axis). The reduction of inertia per unit meter is presented in Fig. 9 and Table 4, considering the three bamboo species. Fig. 4 also shows the principal axes angle (θ) from an arbitrarily defined set of axes *Y-Z*. Mean, standard deviation and extreme values for the absolute range of variation per culm is shown in Fig. 10 and Table 4.

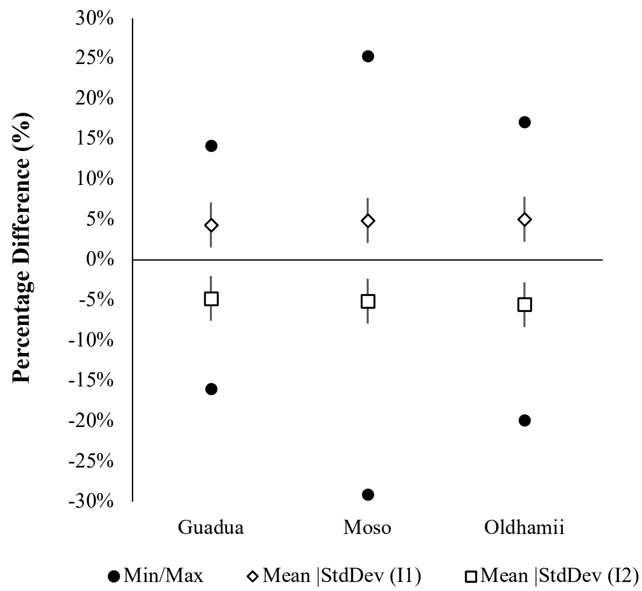

Figure 7. Percentage difference between the actual major (I_1) and minor (I_2) principal moment of inertia and the moment of inertia of an equivalent circular tube

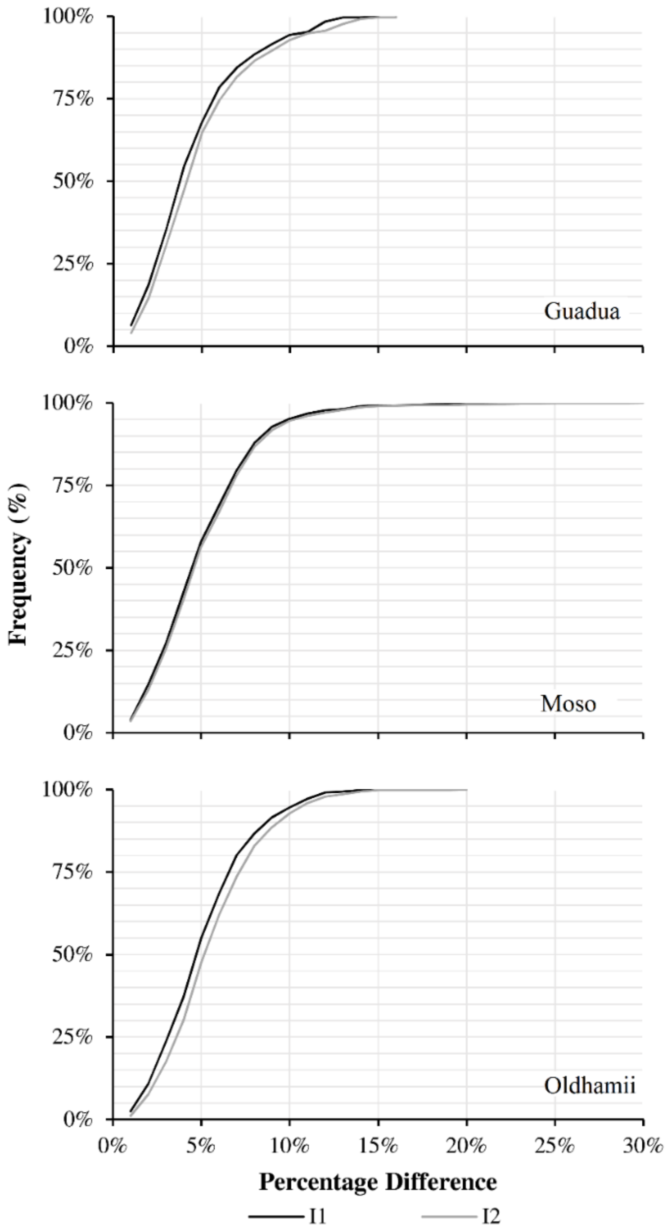

Figure 8. Cumulative frequency distribution for the difference between equivalent inertia and its corresponding major (I_1) and minor (I_2) principal inertia

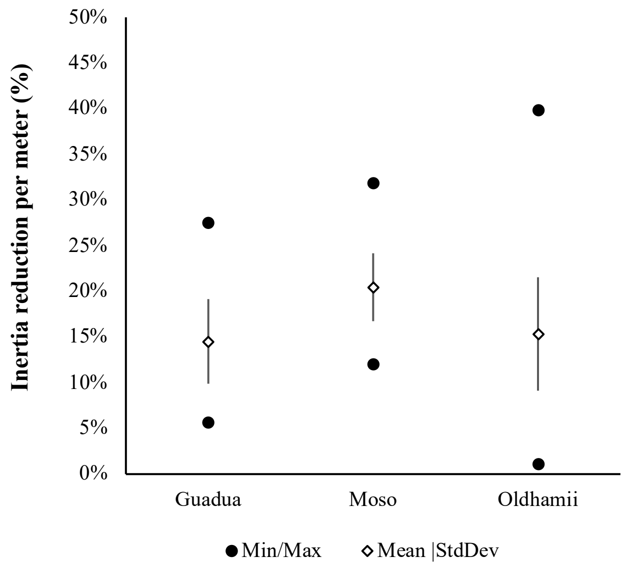

Figure 9. Mean, standard deviation and extreme values of inertia reduction per meter, measured from the bottom end of the bamboo

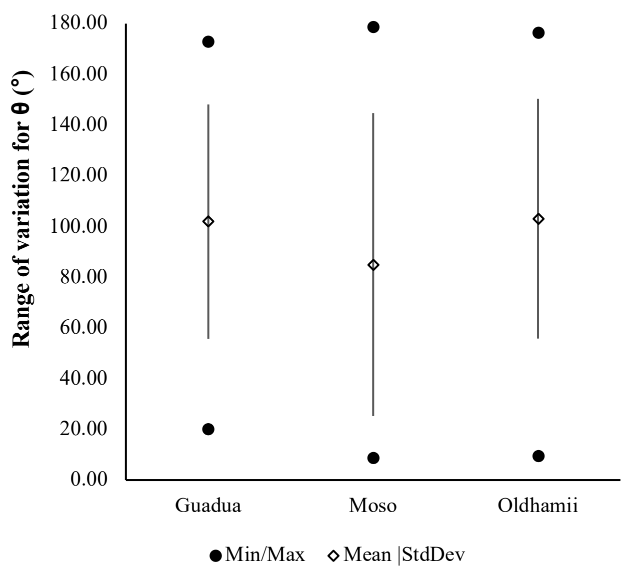

Figure 10. Mean, standard deviation and extreme values for the range of variation of the angle θ

3.2. Correlation analysis

The correlation plot for thickness and diameter is shown in Fig. 11. The variation of these two equivalent properties along the length of the culm is individually computed so that:

Diameter variation (mm/m): $D_v = \frac{\Delta D}{\Delta L}$ (10)

Thickness variation (mm/m): $t_v = \frac{\Delta t}{\Delta L}$ (11)

where ΔD & Δt are the difference in diameter and thickness between the bottom section of each culm and a section at a distance ΔL measured towards the top end of the culm (Fig. 12 & 13 and Table 4).

The Pearson's correlation coefficient was used to measure the statistical correlation between i) equivalent thickness and diameter; ii) diameter (ΔD_i) and length (L_i) and iii) thickness (Δt_i) and length (L_i) as shown in Table 5, together with the coefficient of determination (R^2) of a linear regression on these properties. Common statistical methods to find correlation patterns are based on the assumption that the data follows a normal distribution, therefore the acquired database of basic geometric properties of bamboo culms was also tested for departure from normality, according to [37], applying the directional test for skewness and kurtosis. Table 6 shows the results of directional test analysis.

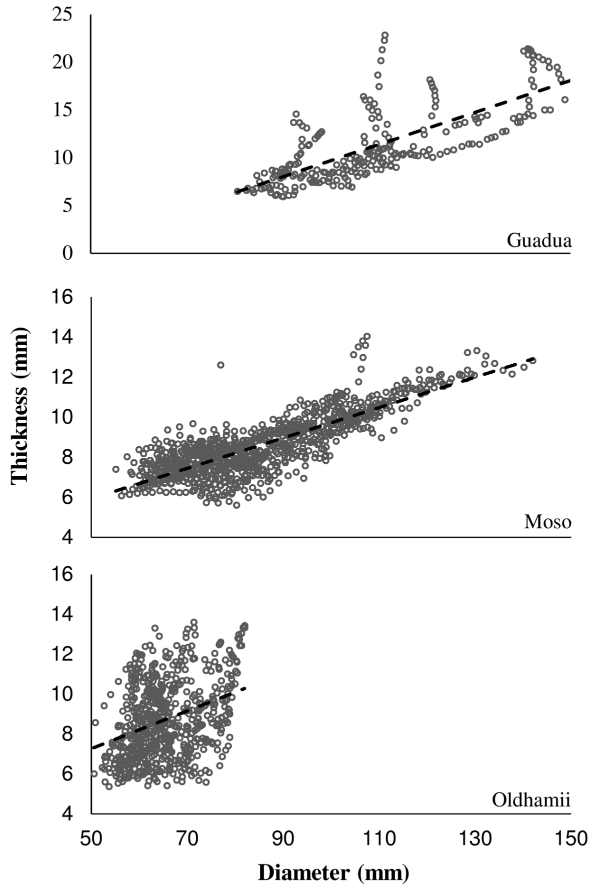

Figure 11. Thickness and diameter correlation for Guadua, Moso and Oldhamii

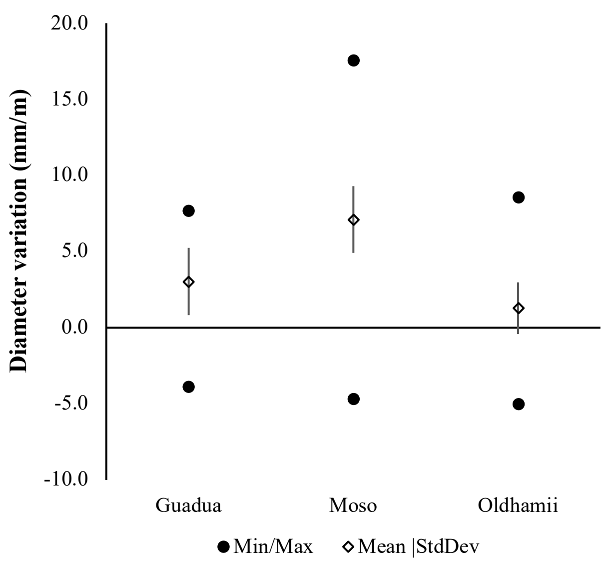

Figure 12. Diameter variation per meter

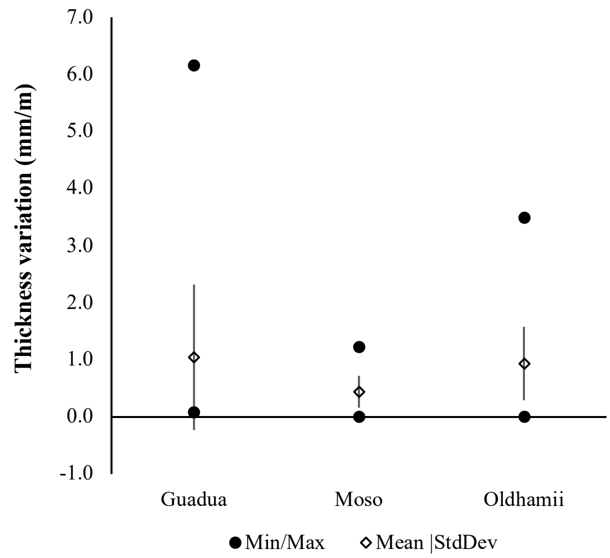

Figure 13. Thickness variation per meter

	Species	Min / Max	Mean	Std. Dev.
Diameter (mm)	Guadua	81 / 151	110	18
	Moso	55 / 142	85	16
	Oldhamii	50 / 82	65	7
Thickness (mm)	Guadua	5.9 / 22.8	11.4	4.0
	Moso	5.6 / 14	8.6	1.5
	Oldhamii	5.4 / 13.6	8.7	1.9
Internodal length (mm)	Guadua	149 / 446	296	69
	Moso	104 / 404	260	56
	Oldhamii	279 / 615	453	64
Out-of- straightness (mm/mm)	Guadua	66 / 478	212	108
	Moso	37 / 529	147	103
	Oldhamii	76 / 771	223	107
% Difference I_1-I	Guadua	0 / 14	4	3
	Moso	0 / 26	5	3
	Oldhamii	0 / 17	5	3
% Difference I_2-I	Guadua	0 / 16	5	3
	Moso	0 / 29	5	3
	Oldhamii	0 / 20	6	3
Inertia reduction (% per m)	Guadua	6 / 28	15	5
	Moso	12 / 32	20	4
	Oldhamii	1 / 40	15	6
θ variation (deg)	Guadua	0 / 180	77	65
	Moso	0 / 180	77	70
	Oldhamii	0 / 180	78	61
Diameter variation (% per m)	Guadua	-4 / 8	3	2
	Moso	-5 / 18	7	2
	Oldhamii	-5 / 9	1	2
Thickness variation (% per m)	Guadua	0 / 6	1.0	1.3
	Moso	0 / 1	0.4	0.3
	Oldhamii	0 / 3	0.9	0.6

Table 4. Numerical summary of results

Method	Thickness to Diameter			Diameter(ΔD) to Length			Thickness(Δt) to Length		
	Guadua	Moso	Oldhamii	Guadua	Moso	Oldhamii	Guadua	Moso	Oldhamii
Pearson	0.76	0.83	0.34	0.75	0.93	0.60	0.08	0.22	0.71
R^2	0.57	0.69	0.11	0.57	0.86	0.36	0.01	0.05	0.51

Table 5. Pearson's correlation and linear coefficient of determination (R^2)

Property		Skewness		Kurtosis	
		Value	Limit	Value	Limit
Guadua	Diameter	0.62		2.44	
	Thickness	0.96	0.25	3.12	2.55
	Internode length	-0.18		2.36	
	Out-of-straightness (δ_r)	0.66	0.66	2.53	1.98
Moso	Diameter	0.65		2.95	
	Thickness	0.74	0.13	3.33	2.76
	Internode length	-0.16		2.51	
	Out-of-straightness (δ_r)	1.84	0.6	6.25	2.35
Oldhamii	Diameter	0.51		2.55	
	Thickness	0.41	0.16	2.37	2.71
	Internode length	-0.11		2.49	
	Out-of-straightness (δ_r)	1.56	0.35	7.64	2.4

Table 6. Departure from normality test for the basic geometric properties

4. Discussion

The digitisation process presented in this study substantially improves the acquisition of the geometric features of bamboo culms through the use of an entry level scanner resulting in high-accuracy 3D models. The applications of digital modelling of bamboo culms are not limited to the scope of this work (geometric analysis) as it allows to extract the relevant information necessary to support the development of, but not limited to, 3D space grid-shells and free-form design, structural analysis, geometric and structural optimisation, material utilisation, construction management and connection design and fabrication. Even though all scanned and processed bamboo culms were selected according to local [16,38,39] and international [14] guidance, as expected, their basic geometric properties still presented a high variability which is likely to increase as the sample size grows [40], especially when culms are not subjected to specific and time-consuming visual examinations. However, average results shown in Fig. 6 are in accordance with the geometric properties found in the literature for the studied species and corresponding sections of the plant.

Bamboo NURBS models were particularly useful to enable the accurate and systematic measurement of the out-of-straightness of the culms which is fundamental to determine their load carrying capacity [11,12,17]. These culms are organic structural elements whose centroid shows a continuous spatial variability (not a straight line) and are cut to any length according to the building requirements. Therefore, the out-of-straightness (δ_r) of the final, cut-to-size, structural culm is a more relevant structural parameter than that of harvested culms of arbitrary lengths. Fig. 14 shows an example where a shorter length within a harvested culm (L_b) produces a more critical out-of-straightness ratio than the original harvested length (L_a). Associating an out-of-straightness (δ_r) value to a harvested culm is therefore not appropriate for any grading or selection process, so that each structural element should be assessed depending on its final length. For example, if the harvested length of the studied culms is considered to assess their suitability as structural members according to the out-of-straightness limit proposed for each species (Table 1), 80% of the Guadua and 40% of the Moso culms would be rejected. The average (± standard deviation) out-of-straightness ratios (δ_r) obtained using the culms' harvested length (Eq. 9) were 212±108, 147±103 and 223±107 for Guadua, Moso and Oldhamii respectively.

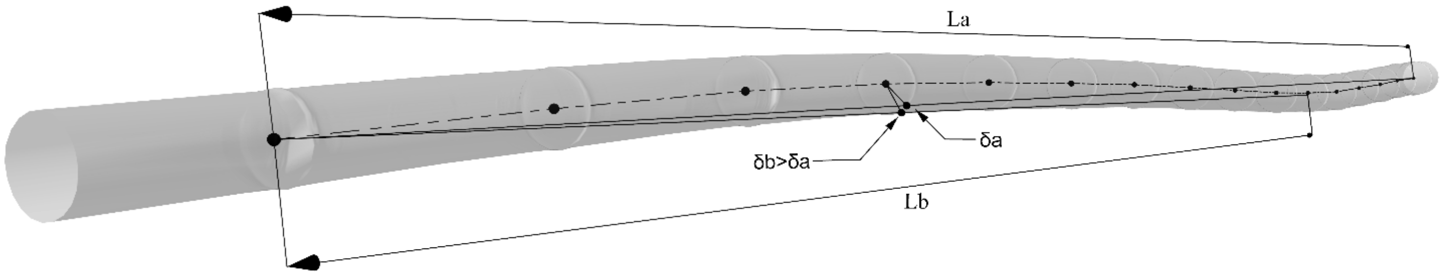

Figure 14. Spatial out-of-straightness of a bamboo culm

4.1. Cross-section properties

In average, actual cross section properties differed 5% from the equivalent properties (Fig. 7), however, the percentage of culms having an equivalent cross-section deviating 5% or more from the actual property was 35%, 42% and 45% for Guadua, Moso and Oldhamii respectively (Fig. 8). This deviation of cross-sectional properties is directly related to the irregularity of the actual tubular shape. The average reduction in inertia per unit meter along the pole was, 15% for Guadua and Oldhamii and 20% for Moso (Fig. 9, Table 4). This effect is not only related to the reduction in diameter and thickness along the pole (taper) but also to the change of cross-sectional shape which was observed to have a random distribution. This random distribution in the cross-sectional shape is reflected in the wide range of angles (θ) at which the principal moments could be found along a single a culm as shown by the standard deviations in Fig. 10. The structural implications of the variation in cross-sectional properties is still under study [11,42,43], therefore accurate and systematic methods to measure these properties and assess their variability are necessary to continue improving our understanding of bamboo as a structural element.

4.2. Correlation analysis

The inherent variation in the geometric properties of bamboo culms needs to be studied to determine potential correlation patterns among these properties that could help define possible grading and quality assurance systems. For example, the thickness shows a tendency which is directly proportional to the diameter (Fig. 11), however the individual variability of these two properties reduces the possibility of a strong correlation pattern (Fig. 12 and 13). In some instances, bamboo culms from all three species presented an increase in equivalent diameter towards the top end, when a reduction is commonly expected (Fig. 12). The coefficients of correlation obtained (Table 5) indicated that only the diameter and length of Moso had a strong correlation (Pearson=0.93, R2=0.86), which is similar to other findings [11] which employed manual measurement methods to acquire basic geometric properties. This result is far from conclusive as Moso is only one of the many potential species suitable for construction and results from this work can only be related to Moso bamboo with similar characteristics. Normally distributed data is a basic assumption necessary to apply correlation tools to develop models that describe variables, but the basic geometric properties studied did not always follow a normal distribution (Table 6). The study of the significance and applicability of this deviation from normality to this and other species is beyond the scope of this work and should be examined based on further datasets.

5. Conclusion

The inherent geometric irregularity of bamboo culms is one of the main challenges for their integration into formal design and fabrication processes in the construction industry. The limitations of manual measuring techniques based on analogue tools can be overcome through the reverse engineering approach presented in this study which, based on 3D scanning and digital modelling tools, can efficiently and accurately capture the organic geometry of bamboo culms. This approach has been applied to capture the geometric data of 235 culms of three different bamboo species and generate their corresponding NURBS-surface models and numerical databases to determine their fundamental geometric properties. Due to the non-destructive nature of the scanning process and based on previous evidence, the internal bamboo surface in these models has been generated based on a linear interpolation of the scanned wall thickness at the end-sections of the culms. This work presents the results of a comprehensive analysis of these geometric properties including the study of any potential correlation among them. The results of this study showed that the basic geometric properties of culms have a wide range of variability without any clear correlation patterns that could be adopted as potential grading or quality assurance systems. A clear understanding of the geometric variability of bamboo culms can support their widespread utilisation in construction through new formal design and construction processes suitable for these natural structural elements. The proposed reverse engineering methodology adopted for this study has the potential to support these new processes as the degree of geometric variability of bamboo culms seems to be incompatible with some of the traditional process developed for manufactured structural elements.

6. Acknowledgements

The authors would like to thank Dr Gerardo Oliva-Salinas and Mr David Trujillo for enabling the procurement of the bamboo used in this study as well as Dr Chuhee Lee for her support during the digitisation programme.
Funding: This work was supported by the UK Engineering and Physical Sciences Research Council (EPSRC) [grant numbers: EP//M017702/1 & EP/P510890/1]; and the British Council/CSC UK-China Joint Research and Innovation Partnership Fund [grant number: UK-276080305].

7. References

[1] J. Allwood, J. Cullen, Sustainable Materials – with Both Eyes Open: Future Buildings, Vehicles, Products and Equipment, UIT Cambridge Ltd, Cambridge, UK, 2011.

[2] UN-Habitat, 53 UN-Habitat Model Projects, Nairobi, Kenya, 2013.

[3] UN, Transforming our world: The 2030 agenda for sustainable development, US, 2015.

[4] J. Vogtländer, P. Van Der Lugt, H. Brezet, The sustainability of bamboo products for local and Western European applications. LCAs and land-use, J. Clean. Prod. 18 (2010) 1260–1269. doi:10.1016/B978-0-12-375688-6.10082-9.

[5] W. Wu, Q. Liu, Z. Zhu, Y. Shen, Managing Bamboo for Carbon Sequestration, Bamboo Stem and Bamboo Shoots, Small-Scale For. 14 (2015) 233–243. doi:10.1007/s11842-014-9284-4.

[6] E. Zea Escamilla, G. Habert, Environmental impacts of bamboo-based construction materials representing global production diversity, J. Clean. Prod. 69 (2014) 117–127. doi:10.1016/j.jclepro.2014.01.067.

[7] M.S. Vorontsova, L.G. Clark, J. Dransfield, R. Govaerts, T. Wilkinson, W.J. Baker, World checklist of bamboos and rattans, International Network for Bamboo and Rattan, Beijing, China, 2016. http://apps.kew.org/wcsp.%0AHow.

[8] S. Kaminski, A. Lawrence, D. Trujillo, Structural use of bamboo Part 1 : Introduction to bamboo, Struct. Eng. (2016) 40–43.

[9] S. Amada, Y. Ichikawa, T. Munekata, Y. Nagase, H. Shimizu, Fiber texture and mechanical graded structure of bamboo, Compos. Part B Eng. 28 (1997) 13–20. doi:10.1016/S1359-8368(96)00020-0.

[10] K.F. Chung, W.K. Yu, Mechanical properties of structural bamboo for bamboo scaffoldings, Eng. Struct. 24 (2002) 429–442. doi:10.1016/S0141-0296(01)00110-9.

[11] K.A. Harries, J. Bumstead, M. Richard, D. Trujillo, Geometric and material effects on bamboo buckling behaviour, Proc. Inst. Civ. Eng. - Struct. Build. 170 (2017) 236–249. doi:10.1680/jstbu.16.00018.

[12] K. Ghavami, L.E. Moreira, The influence of initial imperfections on the buckling of bamboo columns, Asian J. Civ. Eng. (Buillding Housing). 3 (2002) 1–16.

[13] W.K. Yu, K.F. Chung, S.L. Chan, Column buckling of structural bamboo, Eng. Struct. 25 (2003) 755–768. doi:10.1016/S0141-0296(02)00219-5.

[14] ISO 22157-1, International Standard Organization ISO 22157-1. Bamboo-Determination of physical and mechanical properties- Part 1: Requirements, (2004).

[15] M. Richard, Assesing the performance of bamboo sturctural components, University of Pittsburgh, 2013.

[16] NSR-10 G, Reglamento Colombiano de Construcción Sismo Resistente. Título G. Estructuras de Madera y Estructuras de Guagua, (2010).

[17] S. Kaminski, A. Lawrence, D. Trujillo, I. Feltham, L.F. López, Structural use of bamboo. Part 4: Element design equations, Struct. Eng. 95 (2017) 24–27.

[18] EN 1995-1-1, European Standard EN 1995-1-1: 2004. Eurocode 5: Design of timber structures - Part1-1: General- Common rules and reuls for buildings, (2004).

[19] W. Boehler, A. Marbs, 3D Scanning and Photogrammetry for Heritage Recording : a Comparison, in: 12th Int. Conf. Geoinformatics− Geospatial Inf. Res. Bridg. Pacific Atl., University of Gävle, Sweden, 2004: pp. 291–298.

[20] N.J. Shih, H.J. Wang, C.Y. Lin, C.Y. Liau, 3D scan for the digital preservation of a historical temple in Taiwan, Adv. Eng. Softw. 38 (2007) 501–512. doi:10.1016/j.advengsoft.2006.09.014.

[21] W. Bin Yang, M. Bin Chen, Y.N. Yen, An application of digital point cloud to historic architecture in digital archives, Adv. Eng. Softw. 42 (2011) 690–699. doi:10.1016/j.advengsoft.2011.05.005.

[22] C. Thomson, J. Boehm, Automatic Geometry Generation from Point Clouds for BIM, Remote Sens. 7 (2015) 11753–11775. doi:10.3390/rs70911753.

[23] B. Conde, A. Villarino, M. Cabaleiro, D. Gonzalez-Aguilera, Geometrical issues on the structural analysis of transmission electricity towers thanks to laser scanning technology and finite element method, Remote Sens. 7 (2015) 11551–11569. doi:10.3390/rs70911551.

[24] G. Castellazzi, A.M. D'Altri, G. Bitelli, I. Selvaggi, A. Lambertini, From laser scanning to finite element analysis of complex buildings by using a semi-automatic procedure, Sensors (Switzerland). 15 (2015) 18360–18380. doi:10.3390/s150818360.

[25] R. Lorenzo, C. Lee, J.G. Oliva-Salinas, M.J. Ontiveros-Hernandez, BIM Bamboo: a digital design framework for bamboo culms, Proc. Inst. Civ. Eng. - Struct. Build. 170 (2017) 295–302. doi:10.1680/jstbu.16.00091.

[26] K. Crolla, Building indeterminacy modelling – the 'ZCB Bamboo Pavilion' as a case study on nonstandard construction from natural materials, Vis. Eng. 5 (2017) 15. doi:10.1186/s40327-017-0051-4.

[27] C. Hong, H. Li, R. Lorenzo, G. Wu, I. Corbi, O. Corbi, Z. Xiong, D. Yang and Huizhong Zhang, Review on Connections for Original Bamboo Structures, J. Renew. Mater. 7 (2019) 713–730. doi:10.32604/jrm.2019.07647.

[28] R. Lorenzo, L. Mimendi, Digital workflow for the accurate computation of the geometric properties of bamboo culms for structural applications, in: ACEM2018 and SBMS1, 2019: pp. 1–11. doi:https://doi.org/10.1051/matecconf/201927501024.

[29] Wikipedia, Polygon Mesh, (2019). https://en.wikipedia.org/wiki/Polygon_mesh (accessed January 24, 2019).

[30] Wikipedia, Non-uniform rational S-spline, (2019). https://en.wikipedia.org/wiki/Non-uniform_rational_B-spline (accessed January 24, 2019).

[31] Artec 3D, (2019). https://www.artec3d.com/ (accessed January 24, 2019).

[32] Wikipedia, Point Cloud, (2019). https://en.wikipedia.org/wiki/Point_cloud (accessed January 24, 2019).
[33] RMNA, Robert McNeel & Associates- Rhinoceros 3D. Software Version 5.0, (2015).
[34] Rhino.Python, (2019). https://developer.rhino3d.com/guides/rhinopython/ (accessed January 24, 2019).
[35] T.S.S. Paraskeva, G. Grigoropoulos, E.G.G. Dimitrakopoulos, Design and experimental verification of easily constructible bamboo footbridges for rural areas, Eng. Struct. 143 (2017) 540–548. doi:10.1016/j.engstruct.2017.04.044.
[36] BS EN 1310, British adoption of European Standard BS EN 1310: 1997. Round and sawn timber - Method of measurement of features, (1997).
[37] BS 2846-7, British Standard BS 2846-7:1997. Guide to Statistical interpretation of data, (1997).
[38] P. Luna, C. Takeuchi, G. Granados, F. Lamuns, J. Lozano, Metodología de diseño de estructuras en guadua angustifolia como material estructural por el método de esfuerzos admisibles, Rev. Educ. En Ing. 11 (2011) 66–75.
[39] J.M. Ubidia, Construir con Bambú Manual de construcción, 3rd ed., INBAR, 2015, 2015.
[40] M.F. Ashby, L.J. Gibson, U. Wegst, R. Olive, The Mechanical Properties of Natural Materials. I. Material Property Charts, Proc. R. Soc. A Math. Phys. Eng. Sci. 450 (1995) 123–140. doi:10.1098/rspa.1995.0075.
[41] E.T. Bahtiar, N. Nugroho, S. Surjokusum, L. Karlinasar, Eccentricity Effect on Bamboo’s Flexural Properties, J. Biol. Sci. 13 (2013) 82–87. doi:10.3923/jbs.2013.82.87.
[42] N. Nugroho, E. Tri Bahtiar, Bamboo taper effect on third point loading bending test, Int. J. Eng. Technol. 5 (2013) 2379–2384.
[43] R. Lorenzo, L. Mimendi, H. Li, Digital analysis of the geometric variability of bamboo poles in bending, in: ACEM 2018 SBMS1, 2019: pp. 1–12. doi:https://doi.org/10.1051/matecconf/201927501007.